AN EXPERIMENTAL STUDY OF ENDWALL HEAT TRANSFER ENHANCEMENT FOR FLOW PAST STAGGERED NON-CONDUCTING PIN FIN ARRAYS

A Thesis

by

VAMSEE SATISH ACHANTA

Submitted to the Office of Graduate Studies of
Texas A&M University
in partial fulfillment of the requirements for the degree of

MASTER OF SCIENCE

May 2003

Major Subject: Mechanical Engineering

AN EXPERIMENTAL STUDY OF ENDWALL HEAT TRANSFER ENHANCEMENT FOR FLOW PAST STAGGERED NON-CONDUCTING PIN FIN ARRAYS

A Thesis

by

VAMSEE SATISH ACHANTA

Submitted to Texas A&M University
in partial fulfillment of the requirements
for the degree of

MASTER OF SCIENCE

Approved as to style and content by:

Sai C. Lau (Chair of Committee)	N. K. Anand (Member)
Y. A. Hassan (Member)	John A. Weese (Head of Department)

May 2003

Major Subject: Mechanical Engineering

ABSTRACT

An Experimental Study of Endwall Heat Transfer Enhancement
for Flow Past Staggered Non-conducting Pin Fin Arrays. (May 2003)
Vamsee Satish Achanta, B. Tech, Indian Institute of Technology, Madras, India
Chair of Advisory Committee: Sai C. Lau

In this work, we analyzed the enhanced heat transfer from the endwall for flow past pin fin arrays. The aim is to resolve the controversy over the heat transfer that is taking place from the endwall and the pin surface.Various parameters were studied and results were obtained. Our results are found to be consistent with some of the results that have been previously published. The results were surprisingly found to be dependent on the height of the pin fin.

To my parents

ACKNOWLEDGMENTS

I would like to thank Prof. Sai C. Lau for his constant help and encouragement throughout the course of this work. I would like to thank Dr. N. K. Anand and Dr. Y. A. Hassan for their help through the work. I would also like to thank Dr. S. W. Moon without whose help this work would not have been completed. I also thank my seniors, Shantanu, Sharat Chandra Prasad and Joel Cervantes for helping me out whenever I was stuck. I would also like to thank Izzy for his help during the preparation of setup and running the experiments. Finally and most importantly, thanks are due to my father, sisters and friends, especially Buggi, for their constant encouragement.

TABLE OF CONTENTS

CHAPTER		Page
I	INTRODUCTION	1
II	LITERATURE SURVEY	6
	A. Effect of Streamwise Spacing (S_L) of Pins	6
	B. Effect of Pin Height (H) on Array-Averaged Heat Transfer	6
	C. Heat Transfer of Pin versus the Endwall	7
	D. Effect of Entrance Length on Heat Transfer	8
III	EXPERIMENTAL SETUP	10
IV	EXPERIMENTAL PROCEDURE	13
V	DATA REDUCTION	15
VI	RESULTS AND DISCUSSION	17
	A. Effect of Reynolds Number Re_{Dh}	17
	B. Effect of Height of Pins, H/D	21
	C. Effect of Stream Wise Spacing of Pins, S_L/D	21
	D. Effect of Transverse Spacing of Pins, S_T/D	28
	E. Reynolds Dependence of Nusselt Number	28
VII	CONCLUSIONS	34
REFERENCES		35
APPENDIX A		38
APPENDIX B		40
APPENDIX C		42
VITA		43

LIST OF FIGURES

FIGURE		Page
1	Typical Pin Fin Configuration	2
2	Streamwise (S_L) and Transverse (S_T) Distances of a Pin Fin Configuration	4
3	Layout of the Experimental Setup	11
4	Effect of Re_{Dh} on Heat Transfer Enhancement for $D = 1.27$cm	18
5	Effect of Re_{Dh} on Increase of Overall Pressure Drop for $D = 1.27$cm .	19
6	Effect of Re_{Dh} on Thermal Performance for $D = 1.27$cm	20
7	Effect of H/D on Heat Transfer Enhancement for $D = 2.54$cm	22
8	Effect of H/D on Increase of Overall Pressure Drop for $D = 2.54$cm .	23
9	Effect of H/D on Thermal Performance for $D = 2.54$cm	24
10	Effect of S_L/D on Heat Transfer Enhancement for D=1.27cm	25
11	Effect of S_L/D on Increase of Overall Pressure Drop for $D = 1.27$cm	26
12	Effect of S_L/D on Thermal Performance for $D = 1.27$cm	27
13	Effect of S_T/D on Heat Transfer Enhancement for $D = 1.27$cm . . .	29
14	Effect of S_T/D on Increase in Overall Pressure Drop for $D = 1.27$cm	30
15	Effect of S_T/D on Thermal Performance for $D = 1.27$cm	31

CHAPTER I

INTRODUCTION

In the modern world, to achieve high thermal efficiencies, gas turbines are run at pressures and temperatures which are beyond the metallurgical limits of the turbine components. To prevent the advanced material fatigue or degradation, cooling schemes are required to cool the hot sections. Pin fin arrays are one of the most common geometry used to increase the internal heat transfer to a turbine blade or vane and hence help maintain the blade temperature below the allowable limits. It was found that staggered pin fin configuration gives more heat transfer enhancement relative to inline pin fin configuration. The typical configuration of pin fins in a staggered arrangement is shown in Fig 1.

The pin fin arrays are an array of short cylinders which span the cooling flow passage. They increase the internal wetted surface area and also increase the flow turbulence. The pin fins usually used for turbine cooling have a height to diameter ratios H/D between 1/2 and 4 due to the blade size and manufacturing constraints. [1]. Arrays of long cylinders $H/D < 8$ have been used in heat exchanger industry. The heat transfer in long pin arrays is dominated by the cylinders while the endwall effects have been shown to be secondary [2]. In short pin fins the flow across the cylinder is highly influenced by the endwall [3]. The heat transfer in this case is dominated by the endwalls and the pins affect the surface area exposed. Thus the short pin fins have to be studied in order to get the correct estimate of physics taking place rather than an interpolation of the intermediate-sized pin fins used in turbine blades and vanes [4]. The heat transfer in the turbine pin fin arrays is a combination of the

---

The journal model is *IEEE Transactions on Automatic Control.*

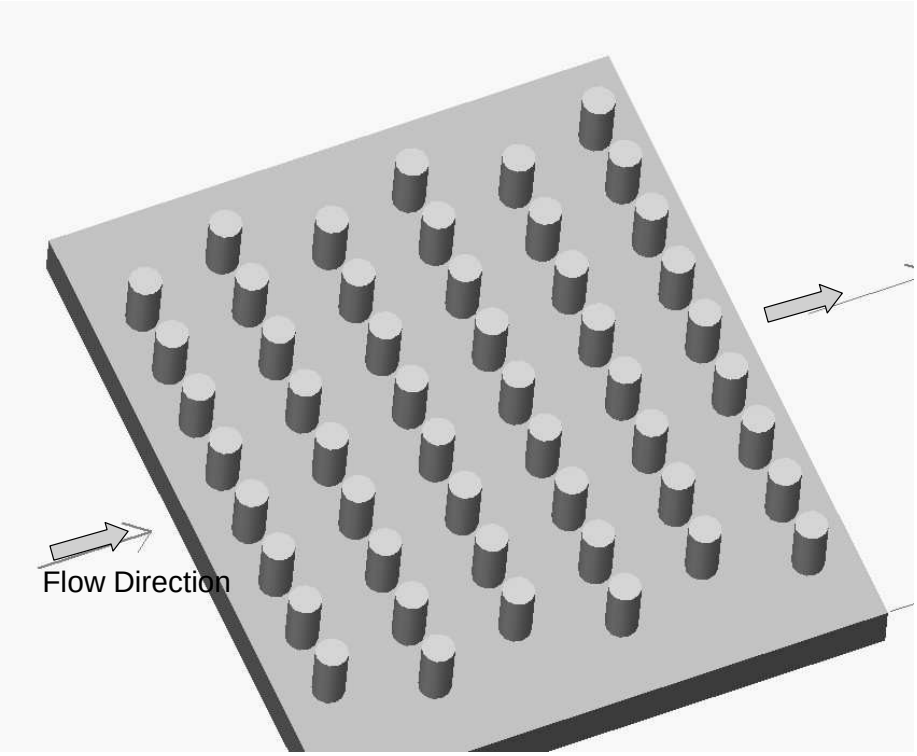

Fig. 1. Typical Pin Fin Configuration

pin heat transfer and the endwall heat transfer. The endwall heat transfer is greatly enhanced when compared to the smooth wall case without any pins. The pins break up the flow taking place, thus increase the turbulence. The pin heat transfer is greatly influenced by the pin-endwall interactions. Sparrow et al. [5]. used a long cylinder attached to a wall in crossflow to study the cylinder endwall interaction. Using both flow visualization and naphthalene mass transfer technique, Sparrow showed that the wall cylinder interactions were confined to the within a diameter of the wall. The effect of the wall was shown to decrease the nearwall cylinder heat transfer compared to the heat transfer away from the wall where the cylinder is unaffected by the endwall. Thus it can be concluded that the average pin heat transfer for relatively short pins in turbines should be lower than long cylinder heat transfer rates. The typical flow regime occurs between , where the boundary layer around the cylinder contains both laminar and turbulent regions. This is the operating regime associated with the turbine blade cooling [4]. Both cylinder vortex shedding and turbulent production occur within this range. VonFossen [6] published an early paper on pin fin cooling in staggered arrays. The two geometries he studied were $H/D = 1/2$, $S_T/D = 1.732$, $S_L/D = 2.0$ and $H/D = 2$, $S_T/D = 3.464$, $S_L/D = 4.0$. Metzger and associates [7, 8, 9, 10] have done extensive studies of pin fin arrays with $H/D = 1.0$ and $S_T/D = 2.5$. Metzger and Shepard [10] correlated the effect on heat transfer of streamwise pin spacing, for geometries varying from $S_L/D = 1.5$ to $S_L/D = 5$ see Fig. 2. The data was correlated and after accounting for difference in number of rows averaged, predicted VanFossen's data well and was stated to be good for $0.5 < H/D < 3.0$. Further studies were done by Armstrong and Winstanley [4] and Chyu et al.[11, 12] for staggered pin fin configurations. All these studies investigated the effects of pin geometry, array geometry, flow parameters and thermal conditions. Heat transfer results obtained include array-averaged $Re - Nu$ correlations and row-

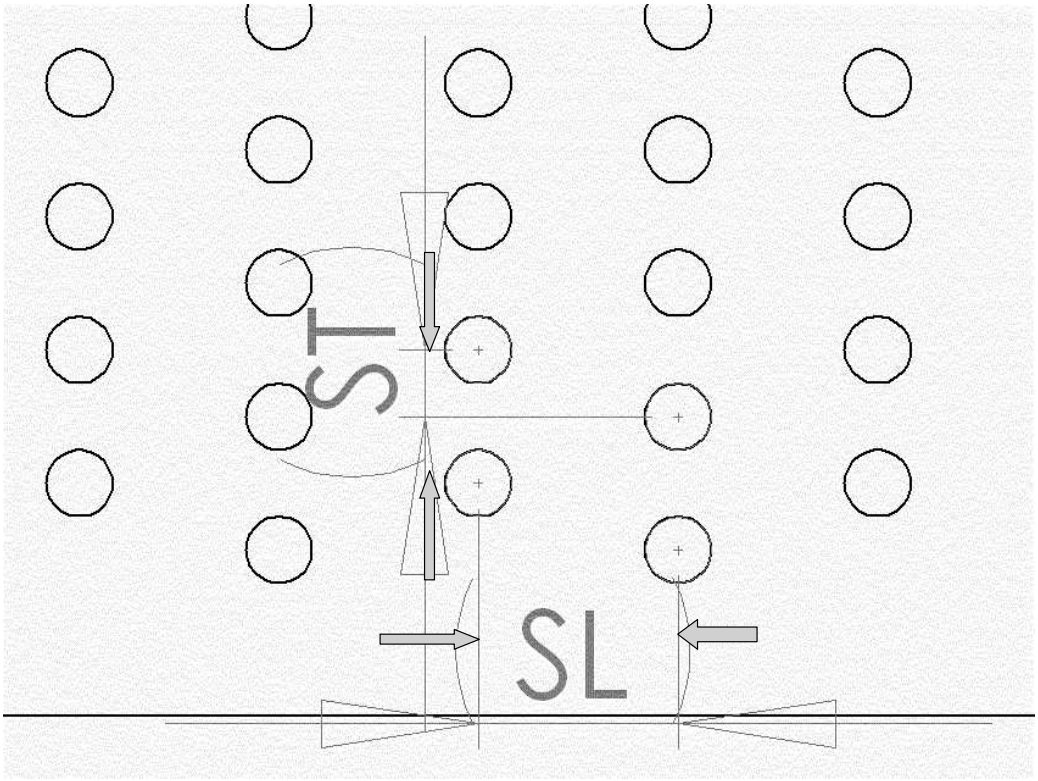

Fig. 2. Streamwise (S_L) and Transverse (S_T) Distances of a Pin Fin Configuration

resolved heat transfer distributions. Beside the total heat transfer that is taking place from the configuration, the amount of heat transfer taking place from pins only and the uncovered endwalls has always been of great importance. There were some studies in recent years to determine the percentage of heat transfer shared by the pins and the uncovered endwalls, however these studies have produced very different results. VanFossen [6] found that the heat transfer coefficient on the pin surface is about 35 percent higher than the heat transfer coefficients on the endwalls. Metzger et al.[9] found that the pin surface heat transfer is double that of the endwalls which is very different from that found by VanFossen [6]. Chyu et al.[11] found that the heat transfer coefficients for the pin surface and endwalls have comparable values. Many studies [see 13-20] have been conducted for short pin fin staggered arrays for various configurations and H/D values. But the inconsistency in the amount of heat transfer share between the pins and endwall is yet to be accounted for. This experiment aims at finding accurate results of heat transfer that take place from the endwalls only and hence help to determine the percent of heat transfer taking place from the endwalls by comparing the results against the total heat transfer taking place from the vast data available. A parametric study is conducted with varying pin fin configuration both in the flow direction and the transverse direction and for two pin heights for different Reynolds number.

CHAPTER II

LITERATURE SURVEY

The various parameters attempted to study are the streamwise pin spacing, S_L/D, transverse pin spacing, S_T/D, height of the pin fin arrays, H/D and the flow velocities, Re_D. The endwall heat transfer and the frictional losses for the pin fin arrays are studied. The predicted endwall heat transfer variation with each of the parameter variation is explained below.

A. Effect of Streamwise Spacing (S_L) of Pins

Metzger et al [8] conducted experiments using the non conducting wooden pins. The study found that the heat transfer varies significantly with streamwise spacing. Increasing the streamwise spacing of pins resulted in a decrease of heat transfer. The difference between the closely placed pins ($S_L/D = 1.05$) and the most widely spaced pin array ($S_L/D = 5$) was approximately 100 percent at $Re_D = 10^3$. This difference decreased to 50 percent at $Re_D = 10^5$.

B. Effect of Pin Height (H) on Array-Averaged Heat Transfer

Brigham and VanFossen [21] investigated the effect of pin height on array-averaged heat transfer. The results show that for H/D less than three, there is no effect of H/D on array-averaged heat transfer. For H/D greater than three the heat transfer significantly increases with increasing H/D. A physical explanation for this observation is given by Armstrong and Winstanley [4]. For short pins, the endwalls compose a significant portion of the heat transfer surface. The pin heat transfer is dominated by the endwall interactions. The scale of the turbulent vortices can be expected to

be of the order of the pin diameter, which is of the same order of the height of the channel for short pins. The flow will be well mixed with no separation of wall and pin effects. As the pins lengthen, a greater percentage of the surface area is comprised by the pin. Endwall-pin interactions no longer dominate the flow near the center of the channel. This is consistent with the previously mentioned observations of Sparrow et al. [5], where a cylinder is affected by the endwall on the order of one diameter away from the wall.

C. Heat Transfer of Pin versus the Endwall

The pin heat transfer has been studied without the endwall effects which will be similar to the cylinder heat transfer in crossflow. The studies of Zukauskas[2], Simoneau [13] and Metzger [7] got consistent results. Heat flux measurements in all above studies were not made at the end of the pins to study the endwall effects. VanFossen [6] studied the average heat transfer effects of the first four rows of pins in a staggered pin fin array. Through the use of two different pin materials, copper and wood, the heat transfer coefficient of the pins relative to the endwalls was deduced. VanFossen [6] stated that the pins have a 35 percent higher heat transfer than the endwalls. This claim has never been verified. Metzger [7] studied the endwall heat transfer as compared to the overall pin fin array heat transfer in a staggered pin fin array. They used thermally non-conducting wooden pins and calculated the heat transfer based on the exposed endwall surface area only. They found the endwall heat transfer coefficient to have almost the same level as the combined pin-endwall average. The endwall did show a slightly lower Reynolds number dependence than the overall pin-endwall average for spacing of $S_L/D = 1.5$, $S_T/D = 2.5$, $H/D = 1.0$ and $S_L/D = S_T/D = 2.5$, $H/D = 1.0$. Chyu et al. [11] reported comparable heat

transfer coefficients on the surfaces of the pins and endwall for both in-line and staggered arrays, $S_T/D = S_L/D = 2.5, H/D = 1$. While all pins were made mass transfer active in his study, only one row of the endwall was active during the experiment, so the boundary condition is not a perfect representation of the real situation. Al Dabagh and Andrews [14] employed a transient heating technique to evaluate the heat transfer contributions from the pins and the endwalls. Contradicting all the previous findings, their results indicated that the endwall heat transfer coefficient is 15 to 35 percent higher than the pins. Chyu et al. [12] studied the heat transfer using the mass transfer analogy implementing the isothermal boundary conditions over the entire test section. Their results show that the heat transfer coefficient on the pin surface is higher than that of the uncovered endwall, by approximately 10 to 20 percent. They suggest that the primary cause of such a disagreement is deemed to be a combination of imperfect boundary conditions and measurement techniques that may be insufficient for resolving the highly complex heat transfer characteristics inherited in pin fin arrays. Since in the case of short pin fin arrays the endwall accounts for nearly 80 percent of the wetted area, an experimental approach focused solely on the endwall measurement is expected to give better results. This experimental study is designed on this idea and is aimed to prove the above results or oppose them.

D. Effect of Entrance Length on Heat Transfer

Limited work has been done on the problem of how the entrance flow condition affects the pin fin array heat transfer. Lau et al. [1] made use of the naphthalene mass transfer technique to measure endwall heat transfer in a pin fin array. Two smooth duct entrance lengths of 4 and 21 hydraulic diameters were used to determine how far into the array the entrance condition affects the endwall heat transfer. They found

there was no dependence on entrance effect after the second row. The effect of the entrance length is found to have less penetrating effect due to even pin fin array disturbance and the damping effects of the endwall.

CHAPTER III

EXPERIMENTAL SETUP

The rectangular channel with pin fins in this study models the flow passage between consecutive plate fins in finned tube heat exchangers. The average heat transfer coefficient on the exposed surface of one of the principal walls of the channel is measured for various rates of air flow through the channel. There are two test apparatuses. Each test apparatus consists of an open flow loop with an entrance channel, the test section, a settling chamber, an orifice flow meter, a control valve, and a centrifugal blower (see Fig. 3). The test section and the entrance channel have the same nominal cross section, and both are 22.86 cm (9.0 in.) wide. The distance between the top and bottom walls is either 2.54 cm (1.0 in.) or 3.81 cm (1.5 in.). The test section is 22.86 cm (9.0 in.) long, while the entrance channel is 60.96 cm (24 in.) long. All of the walls of the test section and the entrance channel are constructed of 1.91-cm (0.75-in.) thick plywood, except that the bottom wall of the test section consists of three individual copper segments. The three copper segments are 1.27 cm (0.5 in.) thick and 22.86 cm (9.0 in.) wide, and measure 7.62, 7.46, and 7.62 cm (2.94, 3.0, and 2.94 in.), respectively, along the main flow direction. A 1.59-mm (0.0625-in.) thick wooden gasket separates adjacent copper segments. Attached to the exterior surfaces of the copper segments of the bottom wall is a flexible electric strip heater. During an experiment, heat is supplied to the copper segments from the electric heater and is transferred by convection to the air flowing over the exposed surface of the copper segments. The wooden gasket between adjacent segments minimizes streamwise conduction between the segments. Styrofoam insulation is used to minimize extraneous heat losses. The top wall of the test section also measures 22.86 cm (9.0 in.) along the main flow direction. It consists of a staggered array of holes, through which short

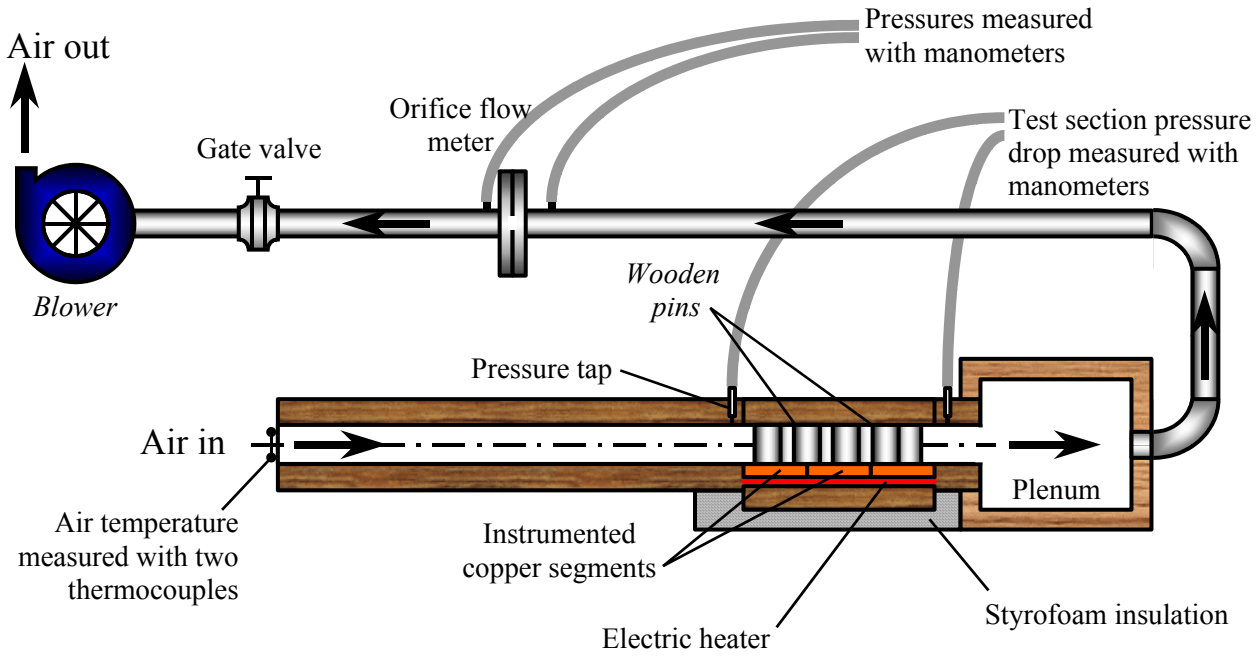

Fig. 3. Layout of the Experimental Setup

wooden cylinders or pins may be inserted. The diameter of the holes and the configuration of the hole array depend on the configuration of the pin fin channel to be studied. Once installed, these wooden cylinders or pins protrude slightly above the outer surface of the top wall. A rubber gasket and a 1.91-cm (0.75-in.) thick wooden board are placed on top of the pins so that pressure may be applied with weights on the wooden board to press the flat bottom surfaces of the pins against the copper bottom wall of the test section.

During an experiment, the power input to the heater is regulated with two variable transformers that are connected in series (one of the transformers limits the maximum power to the heaters). The voltage drop across the heater is measured with a digital multimeter while the current is measured with a current probe and another multimeter. The power input is determined as the product of the voltage drop and the current. Each of the two upstream copper segments in the test section is instrumented with eleven 30-gage, T-type thermocouples to determine the average temperature of the segment during an experiment. Two other thermocouples measure the air temperatures at the inlet of the entrance section. A computer controlled data acquisition system records all thermocouple output. Static pressure taps are installed along the top wooden wall at the inlet and outlet of the test section to determine the pressure drop across the pin fin array during an experiment. An inclined manometer measures the pressure drop across these taps. Another inclined manometer measures the pressure drop across the orifice, and a U-tube manometer measures the pressure upstream of the orifice. These pressures are used to calculate the mass flow rate of air through the test section during an experiment.

CHAPTER IV

EXPERIMENTAL PROCEDURE

The pin configuration to be run was prepared by placing the top wooden plate in its place. The pins corresponding to the drilled configuration diameter and corresponding to the height of the test section to be run were inserted in the wooden plate. Care was taken that the surface of the pin that is to be in contact with the copper plate is a very highly finished flat end. This was required in order not to allow air to pass between the pin end and the copper plate, which if happens would alter the heat transfer area and make calculations difficult or impossible. The other surface of the pin and outer surface of the upper wooden endwall will be in the same plane. The drilled diameter of the bore of the wooden plate and the diameter of the pin is the same so that the gap is between the pins and the bore of the plate is very negligible. This makes the escape of air through the upper endwall difficult. Further care was taken by using duck tape to seal all the open surfaces of the upper endwall to make it leak proof of air. Further a layer of 0.2inch thick insulation was used on top of which a weight of 15kilogram was placed to ensure that the pins sit perfectly on the copper plate and the upper endwall is made sure that it will be leak proof of air.

The blowers were turned on and air was forced through the test setup. The flow rate through the test section could be controlled with the help of a valve downstream of the orifice plate. The flow rate was set in such a way that the pressure drop across the orifice corresponds to the required Reynolds number. After the flow was set across the test section, the heaters were turned on and the voltage supplied to the heaters was roughly set at a value such that the temperature of the copper plates at steady state was to be about 20^0C above the mean bulk temperature of the air. This is to ensure that the heat loss from the test section at the steady state be made as small

as possible and at the same time ensure a sufficient amount of heat transfer from the copper plate to the air is obtained to help calculate the heat transfer coefficient accurately. The temperature difference for every pin configuration was made sure to be about 20^oC so as to make sure that the heat loss from the test section was to be about the same value for all the test runs and hence help get consistent results.

After a time of about 45 to 60 minutes the thermocouple probes in the copper plates reached steady state. The pressure difference across the orifice was checked frequently so that the flow rate did not change from the intended value of Reynolds number. At steady state the temperatures of the thermocouples were noted by the data acquisition system and logged by the computer. The pressure difference across the orifice plate and the pressure across upstream of the orifice plate are measured. The static pressure drop across the test section was measured by connecting the two pressure taps just before the starting of the pin fin configuration to one end of the manometer and another two taps just at the end of the configuration to the other end of the same manometer to give the difference. The voltage supplied to the heater and the corresponding current was taken note to calculate the heat supplied to the copper plates. Two thermocouples placed at the entrance of the test setup measure the inlet temperature of the air.

CHAPTER V

DATA REDUCTION

The Reynolds number for the flow of air through the test section is based on the hydraulic diameter of the test section, D_h and is calculated by

$$Re_{Dh} = \frac{\rho \bar{u} D_h}{\mu} = \frac{\dot{m}}{\mu W} \tag{5.1}$$

where ρ is the density of the fluid and μ is the dynamic viscosity of air, $\dot{m}$ is the mass flow rate of the fluid The average Nusselt number for each of the two copper plates embedded with the thermocouples was calculated separately. The total heat input to all the copperplates is equal to heat input of the silicone heater, Q_{heater}.

$$Q_{heater} = VI \tag{5.2}$$

where V is the voltage and I is the current supplied to the heater and hence the heat to each of the copper plates, Q_{plate} is

$$Q_{plate} = (Q_{heater} - Q_{loss})/3 \tag{5.3}$$

The heat loss q_{loss} is the conduction heat loss through the insulation, which is calculated as

$$q_{loss} = Ak_{ins}(T_w - T_{in})/t_{ins} \tag{5.4}$$

where k_{ins} is the thermal conductivity of the insulation, t_{ins} is the thickness of the insulation

The average wall temperature for each copper plate was found out by averaging the 11 thermocouples placed in each of the copper plates. The bulk temperature of

the air passing each of the copper plate was calculated using the following expression

$$T_{b,i} = T_{in} + \frac{iQ_{plate}}{\dot{m}C_P} \tag{5.5}$$

where T_{in} is the average inlet temperature, C_P is the specific heat capacity of air and i is the number of plate for which the bulk temperature is to be calculated.

As we assumed that each of the two copper plates of interest can be studied as two separate entities separated by wooden splinters. The effective heat transfer coefficient for each plate is calculated from the following expression

$$h_i = \frac{Q_{plate}/A_{effective}}{T_{w,i} - T_{b,i}} \tag{5.6}$$

where $A_{effective}$ is the effective heat transfer area which is calculated as follows

$$A_{effective} = A_{total} - NA_{pin} \tag{5.7}$$

where A_{total} is the area of the plate, N is the number of pins and A_{pin} is the area of cross section of the pins used during the test run.

The average Nusselt number calculated from the above heat transfer coefficient is normalized with the Nusselt number for fully developed turbulent pipe flow, which is calculated using Gnielinski's correlation shown below

$$Nu_{Dh} = \frac{(f/8)(Re_{Dh} - 1000)Pr}{1 + 12.7(f/8)^{1/2}(Pr^{2/3} - 1)} \tag{5.8}$$

where the friction factor f, is given by

$$f = [0.79ln(Re_{Dh}) - 1.64]^{-2} \tag{5.9}$$

Using the data reduction shown above, the Nusselt numbers for four Reynolds numbers and each pin configuration with varying diameter and length of the pins were calculated.

CHAPTER VI

RESULTS AND DISCUSSION

Experimental uncertainties for Nu and Re are estimated to be ±5.39% and ±3.45% respectively, based on methods of Kline and Mclintock [22]. This is a pretty good accuracy for an experimental heat transfer work. The average endwall heat transfer and the pressure drop for turbulent flow past pin fin arrays have been studied for different configurations with varying stream wise and transverse pin distance variations and different diameters for 4 air flow rates, corresponding Reynolds numbers, Re_Dh, of about 6500, 13000, 19500 and 26000.

The results are presented in the form of average Nusselt number ratio Nu_{Dh}/Nu_o and friction factor ratio f/f_o and thermal performance TP. Because of the large pressure drops, the thermal performance was also defined as $(Nu_{Dh}/Nu_o)(f/f_o)^{-1/3}$,whose value was around 1. This gives an estimate of pumping power required to enhance the heat transfer by a unit.

A. Effect of Reynolds Number Re_{Dh}

The variation of the quantities of interest with Re_{Dh}, for cases B, C, F and H are discussed. The trend was the same for all the other cases. Fig. 4 shows that the heat transfer enhancement was the highest of 6.52 for $Re_{Dh} = 6500$ and decreased by 16% for $Re_{Dh} = 13000$ and then decreased by about 6% for $Re_{Dh} = 19500$ and then the decrease for $Re_{Dh} = 26000$ was 1.5% . Fig. 5 shows that the friction factor followed the reverse trend with an increase of 55% for $Re_{Dh} = 13000$ from a value of 85 at $Re_{Dh} = 6500$ and then decreased was 8% for both $Re_{Dh} = 19500, 26000$. Fig. 6 shows that the thermal performance decrease with Re_{Dh} and the decrease was the highest for the lower Reynolds number and followed a faster trend than the heat

transfer enhancement because of increasing friction factor.

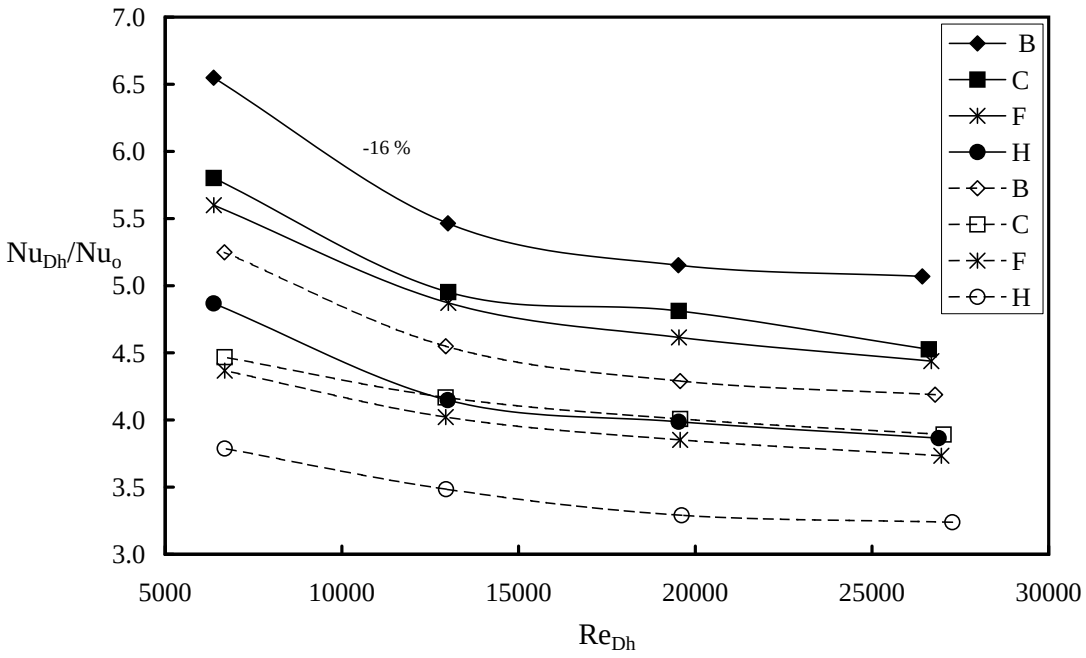

Fig. 4. Effect of Re_{Dh} on Heat Transfer Enhancement for $D = 1.27$cm

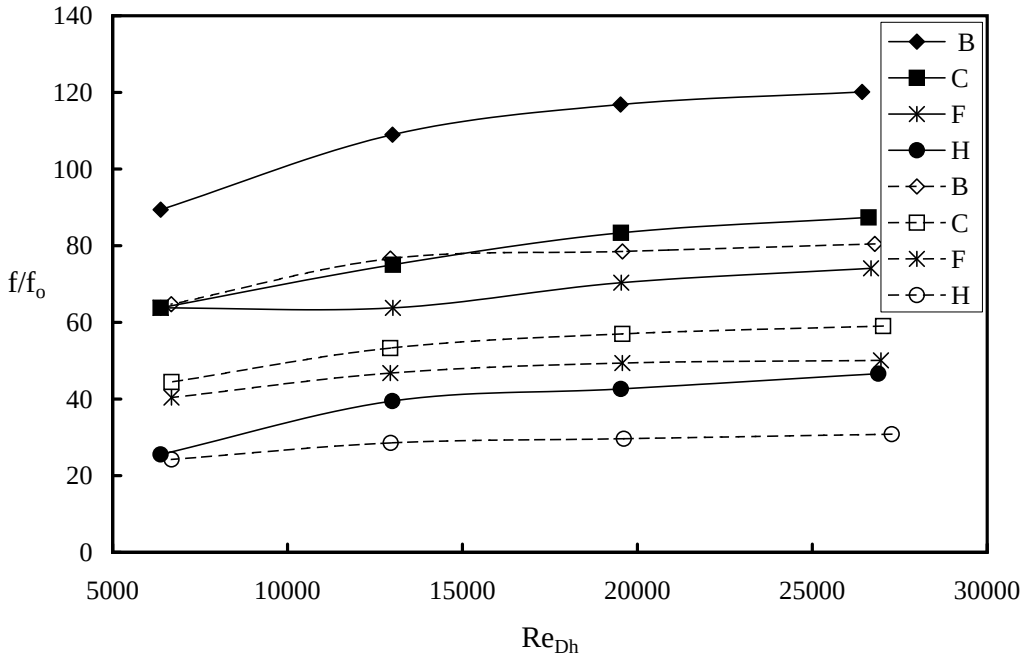

Fig. 5. Effect of Re_{Dh} on Increase of Overall Pressure Drop for $D = 1.27$cm

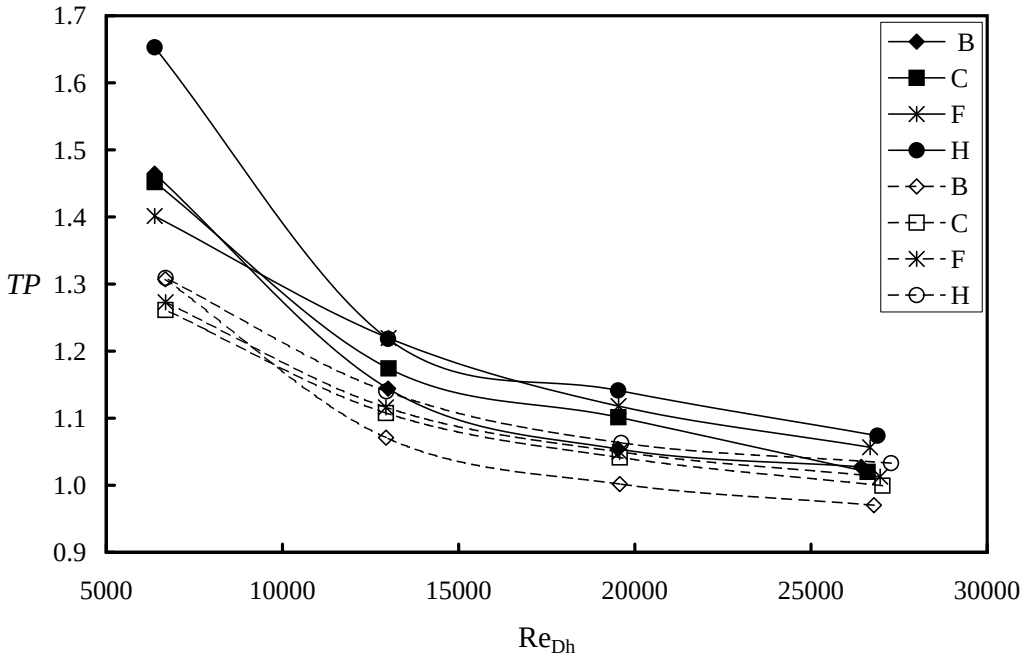

Fig. 6. Effect of Re_{Dh} on Thermal Performance for $D = 1.27$cm

B. Effect of Height of Pins, H/D

The variation of the quantities of interest with H/D, for cases I, J and K are discussed. The trend was the same for all the other similar cases. Fig. 7, Fig. 8 and Fig. 9 illustrate that the increase of H increased the enhancement of endwall heat transfer and the friction losses but increase the thermal performance as well. For case I an increase of H/D from 1 to 1.5 there was an increase of about 34% in heat transfer enhancement forRe_{Dh} = 6500 and the increase was about 26% for all the other Reynolds numbers. The friction factor increased by about 40% to 45% over the Reynolds number range for the same change of H/D for case I.

C. Effect of Stream Wise Spacing of Pins, S_L/D

The variation of the quantities of interest with S_L/D, for cases D, E and F are discussed. The trend was the same for all the other cases. Fig. 10, Fig. 11 and Fig. 12 illustrate that the increase of S_L/D decreased the enhancement of endwall heat transfer and the friction losses. The enhanced Heat Transfer decreased by about 12% from case D, S_L/D = 1.0 to case E, S_L/D = 1.5 for all Reynolds numbers while the pressure loss varied from about 70% to 100% from lower to higher Reynolds number for cases mentioned above. The thermal performance decreased as well but the decrease was not so significant at higher Reynolds number.

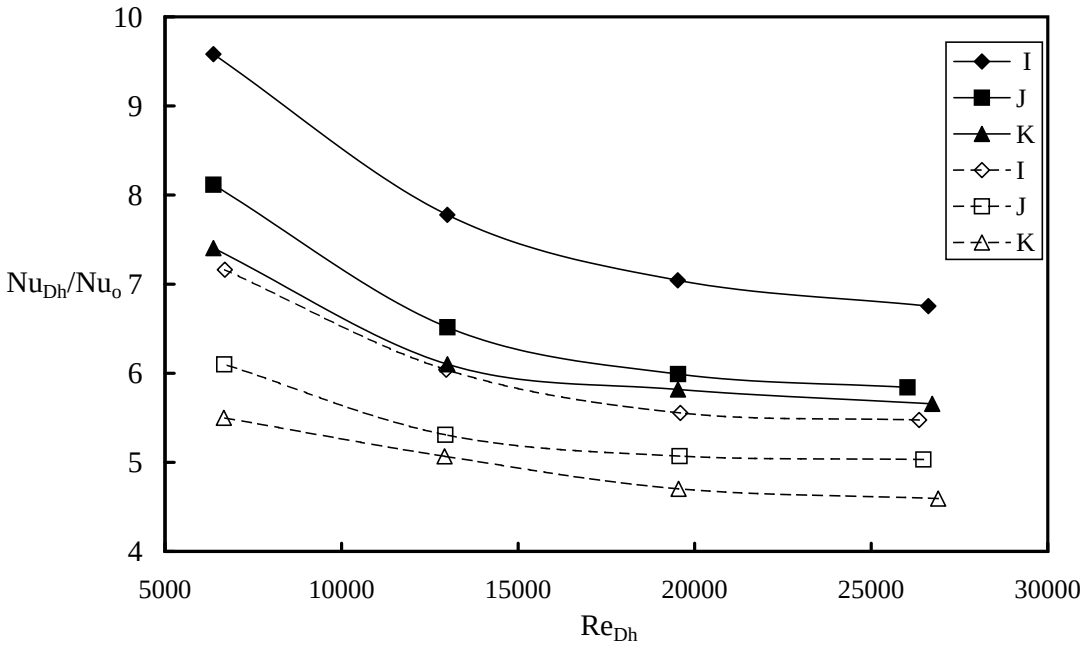

Fig. 7. Effect of H/D on Heat Transfer Enhancement for $D = 2.54$cm

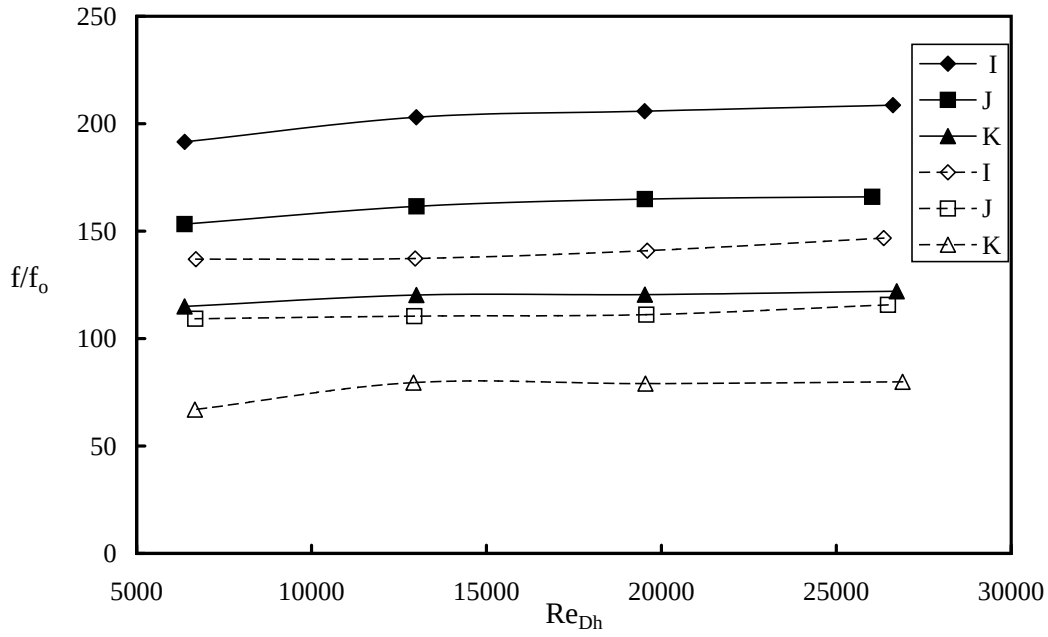

Fig. 8. Effect of H/D on Increase of Overall Pressure Drop for $D = 2.54$cm

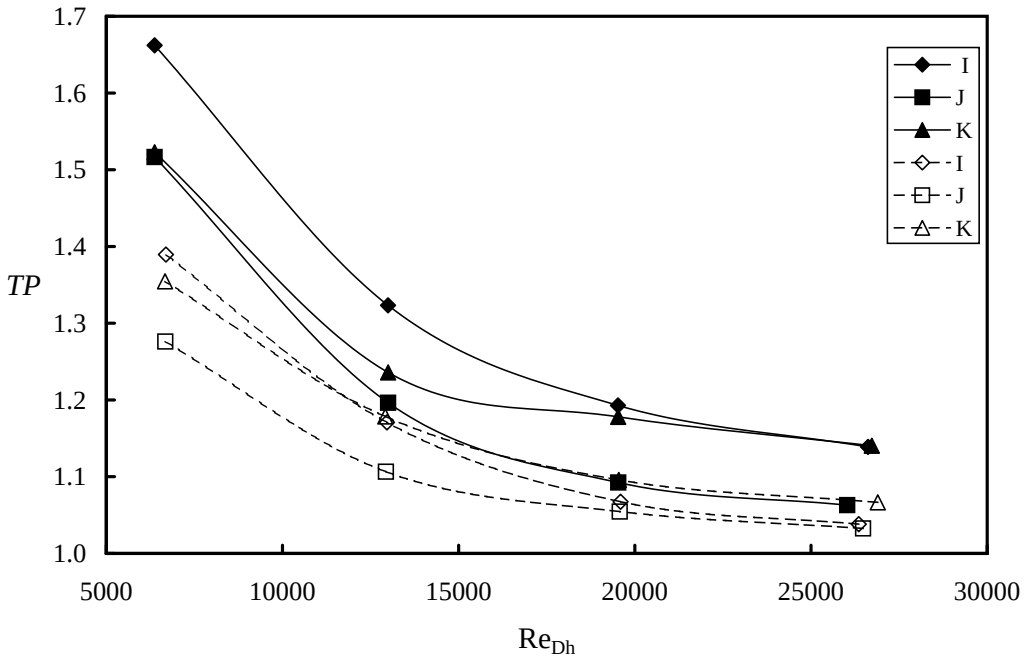

Fig. 9. Effect of H/D on Thermal Performance for $D = 2.54$cm

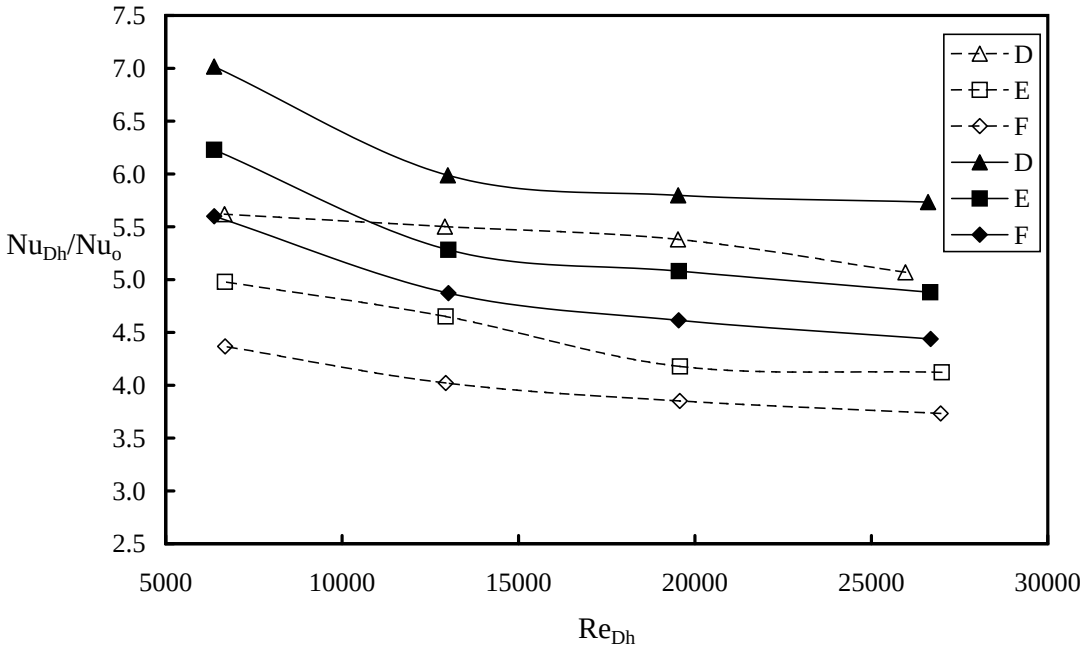

Fig. 10. Effect of S_L/D on Heat Transfer Enhancement for D=1.27cm

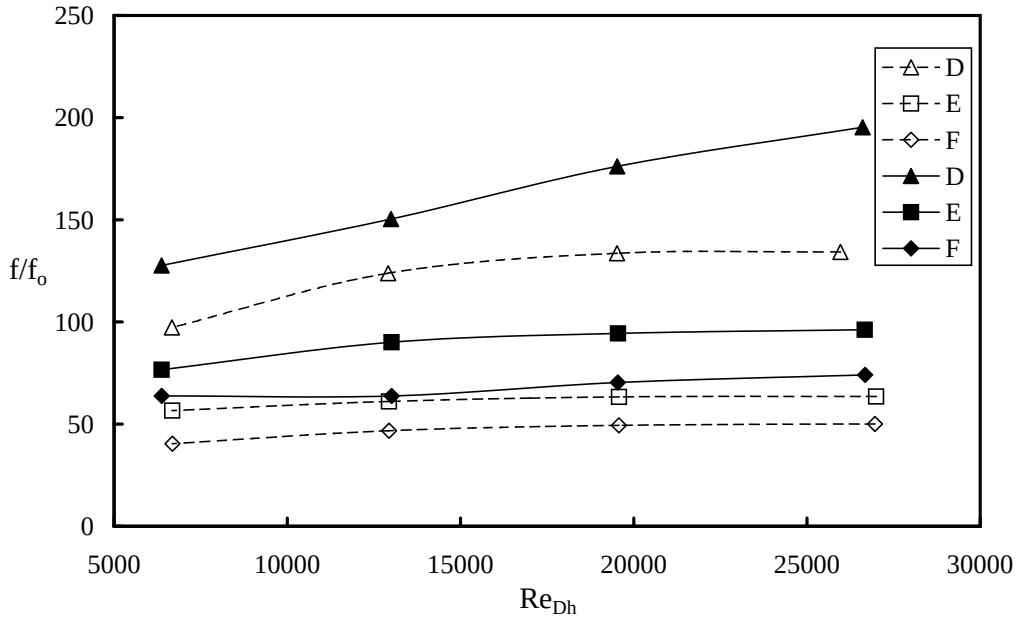

Fig. 11. Effect of S_L/D on Increase of Overall Pressure Drop for $D = 1.27$cm

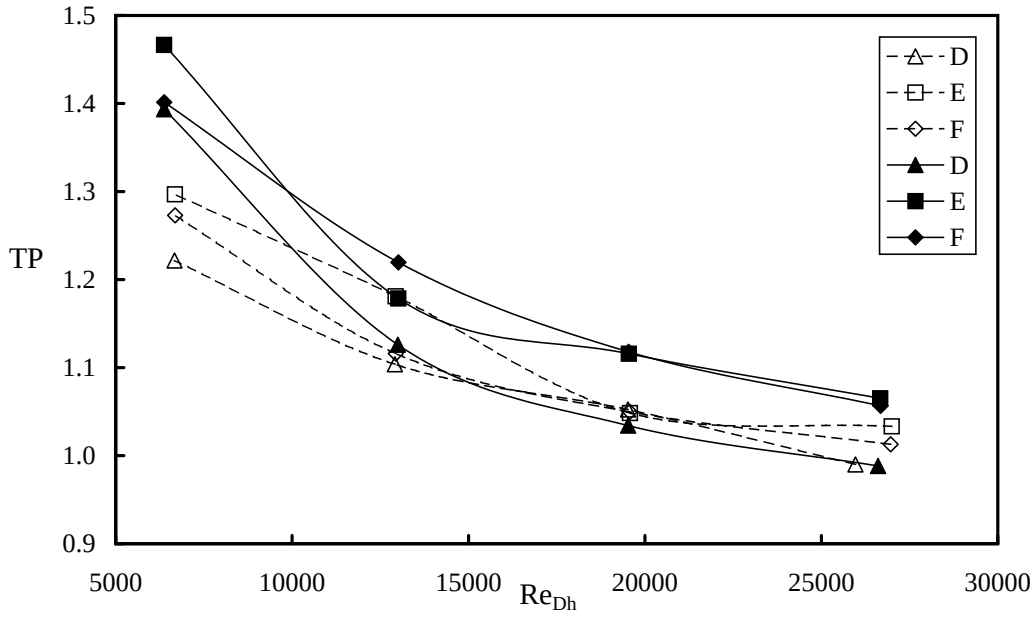

Fig. 12. Effect of S_L/D on Thermal Performance for $D = 1.27$cm

D. Effect of Transverse Spacing of Pins, S_T/D

The variation of the quantities of interest with S_T/D, for cases J, L and N are discussed. The trend was the same for all the other similar cases. Fig. 13, Fig. 14 and Fig. 15 illustrate that the increase of S_T/D decrease the enhancement of endwall heat transfer and the friction losses. The enhanced heat transfer decreased by about 14% from case B, $S_T/D = 2.0$ to case F, $S_T/D = 3$ for all Reynolds numbers while the pressure loss varied from about 40% to 80% from lower to higher Reynolds number for cases mentioned above. It was found that the Transverse spacing of pins had more effect on the enhanced heat transfer than the streamwise spacing. The thermal performance decreased as well but the decrease was not so significant at higher Reynolds number.

E. Reynolds Dependence of Nusselt Number

The Reynolds number dependence of the Nusselt number for each of the case that was examined can be written in the following form as

$$Nu_{Dh} = a{Re_{Dh}}^b \tag{6.1}$$

The log-log graphs of the above graphs were plotted and the coefficients, i.e., a and b for the Reynolds number dependence of the Nusselt number was tabulated in Table 1. It can be deduced from this table that the Reynolds number dependence coefficient, b changes with the H/D ratio and does not follow a particular pattern.

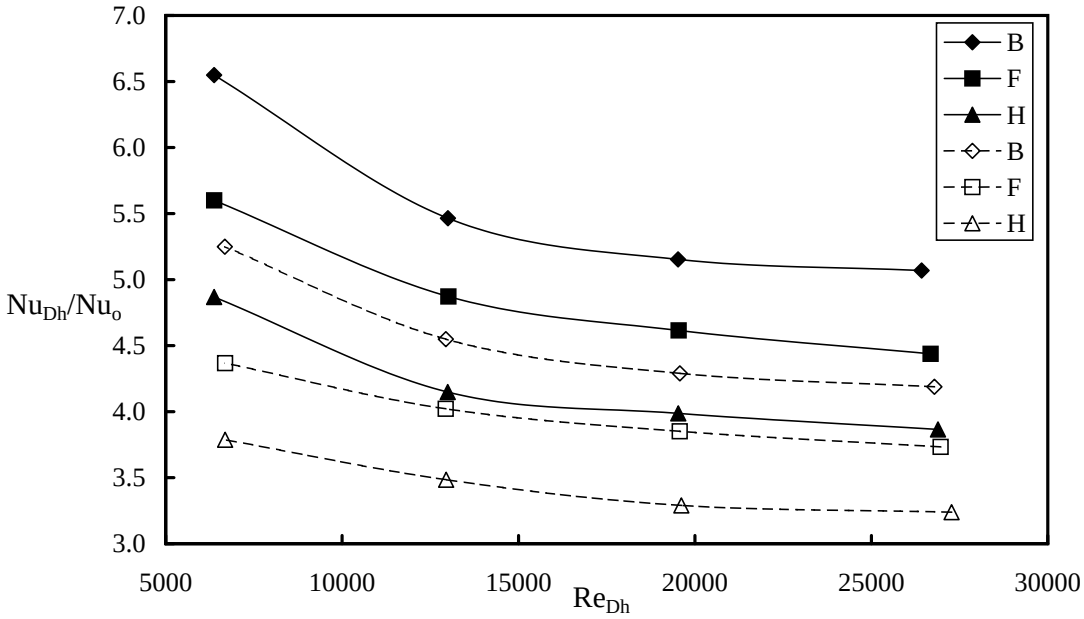

Fig. 13. Effect of S_T/D on Heat Transfer Enhancement for $D = 1.27$cm

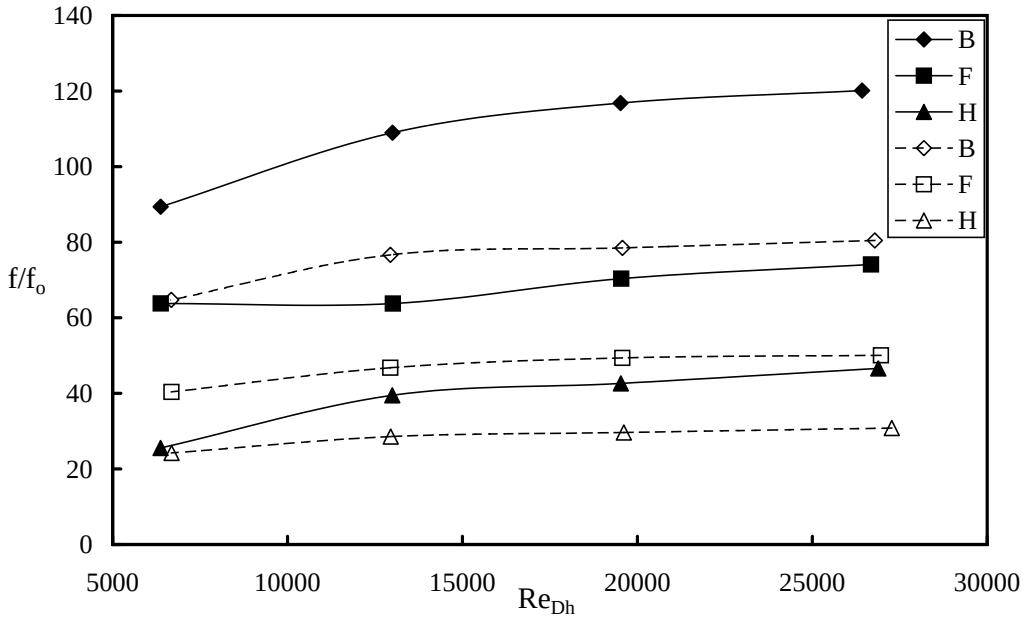

Fig. 14. Effect of S_T/D on Increase in Overall Pressure Drop for $D = 1.27$cm

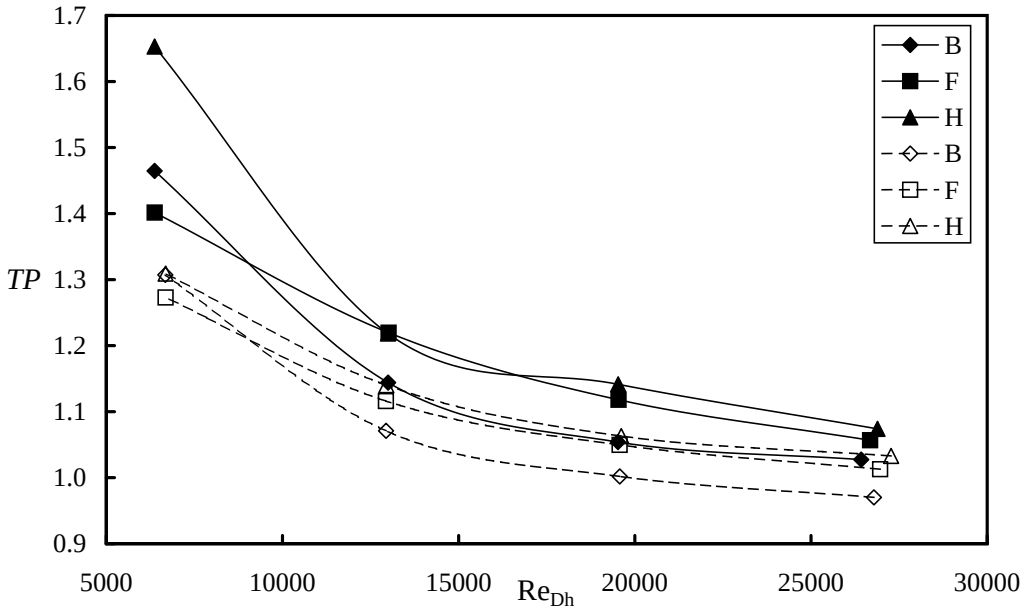

Fig. 15. Effect of S_T/D on Thermal Performance for $D = 1.27$cm

The Reynolds number dependence decreases with increase of H value. The value of b decreases with increase of H for every case. The factor 'a' is a close indicator of what happened to the average Nusselt number we discussed above. That is, when the parameters S_T and S_L changed, 'a' changed accordingly as the average Nusselt ratios changed as shown before.

Table. 1 Dependence coefficients, ‘a’ and ‘b’ of Nusselt number with Reynolds number

Case	D	S_T/D	S_L/D	H	H/D	a	b
B	0.013	2.0	2.0	0.025	2.0	0.44	0.63
				0.038	3.0	0.63	0.61
C	0.013	2.0	3.0	0.025	2.0	0.25	0.67
				0.038	3.0	0.49	0.63
D	0.013	3.0	1.0	0.025	2.0	0.20	0.73
				0.038	3.0	0.47	0.65
E	0.013	3.0	1.5	0.025	2.0	0.36	0.65
				0.038	3.0	0.53	0.63
F	0.013	3.0	2.0	0.025	2.0	0.23	0.68
				0.038	3.0	0.45	0.63
H	0.013	4.0	2.0	0.025	2.0	0.21	0.68
				0.038	3.0	0.38	0.63
I	0.025	1.5	1.0	0.025	1.0	0.84	0.59
				0.038	1.5	1.65	0.55
J	0.025	1.5	1.5	0.025	1.0	0.42	0.65
				0.038	1.5	1.27	0.56
K	0.025	2.0	1.0	0.025	1.0	0.36	0.66
				0.038	1.5	0.75	0.61
L	0.025	2.0	1.5	0.025	1.0	0.33	0.65
				0.038	1.5	0.82	0.58
N	0.025	3.0	1.5	0.025	1.0	0.26	0.66
				0.038	1.5	0.64	0.59
O	0.019	1.3	1.3	0.025	1.3	0.70	0.63
				0.038	2.0	1.49	0.58
P	0.019	4.0	0.7	0.025	1.3	0.24	0.68
				0.038	2.0	0.56	0.60
Q	0.019	2.0	1.0	0.025	1.3	0.54	0.63
				0.038	2.0	0.88	0.60
R	0.019	2.0	1.3	0.025	1.3	0.40	0.65
				0.038	2.0	0.54	0.64
S	0.019	2.0	2.0	0.025	1.3	0.14	0.74
				0.038	2.0	0.60	0.61
U	0.019	4.0	1.3	0.025	1.3	0.20	0.69
				0.038	2.0	0.85	0.71
V	0.019	2.7	1.0	0.025	1.3	0.33	0.68
				0.038	2.0	0.88	0.60
W	0.019	4.0	1.5	0.025	1.3	0.34	0.63
				0.038	2.0	0.44	0.63
X	0.019	2.0	1.5	0.025	1.3	0.61	0.60
				0.038	2.0	0.67	0.61

CHAPTER VII

CONCLUSIONS

An experimental study of the enhanced endwall heat transfer for flow past pin fin arrays has been conducted for turbulent airflow in a rectangular channel with varying configurations of pin fins.

1)The transverse distance had a greater effect on the enhanced heat transfer than the streamwise distance consistent with the previous studies.

2) The Reynolds number dependence of endwall heat transfer was declined with increase of H but did not follow a pattern with varying H/D while all previous studies show that the total heat transfer is independent of H/D. This leads to the conclusion that the decrease in Reynolds number dependence is compensated by an exact increase of the pin wall heat transfer dependence on Reynolds number thus making the total heat transfer constant. More studies of effect of H need to be done in order to get a correct estimate of whether a H/D dimensionless quantity can be formulated in the results.

REFERENCES

[1] Lau, S. C., Kim, Y. S., and Han, J. C., "Effects of Fin Configuration and Entrance Length on Local Endwall Heat/Mass Transfer in a Pin Fin Channel," ASME paper No.85-WA/HT-62., 1985.

[2] Zukauskas, A, "Heat Transfer from Tubes in Crossflow," in *Advances in Heat Transfer*, vol.8, pp. 93-160, 1972.

[3] Webb, R. L., "Air-Side Heat Transfer in Finned Tube Heat Exchangers," *Heat Transfer Engineering*, vol. 1, pp.116-133, 1980.

[4] Armstrong, J., Winstanley, D., "A Review of Staggered Array Pin Fin Heat Transfer for Turbine Cooling Applications," *Journal of Turbomachinery*, vol. 110, pp. 94-103, 1988.

[5] Sparrow, E. M., Stahl, T. J., and Traub, P., "Heat Transfer Adjacent to the Attached End of a Cylinder in Crossflow," *International Journal of Heat and Mass Transfer*, vol. 4, pp. 233-242., 1984.

[6] VonFossen, G. J., "Heat Transfer Coefficients for Staggered Arrays of Short Pin Fins," *Journal of Engineering for Power*, vol. 104, pp. 268-274., 1982.

[7] Metzger, D. E., Berry, R. A., and Benson, J. P., "Developing Heat Transfer in Rectangular Ducts with Staggered Arrays of Short Pin Fins," *Journal of Heat Transfer*, vol. 104, pp. 700-706., 1982a.

[8] Metzger, D. E., and Heley, S. W., "Heat Transfer Experiments and Flow Visualization for Arrays of Short Pin Fins," ASME Paper 82-GT-138, 1982b.

[9] Metzger, D. E., Fan, C. S., and Haley, S. W., "Effects of Pin Shape and Array Orientation on Heat Transfer and Pressure Loss in Pin Fin Arrays," *Journal Engineering for Gas Turbines and Power*, vol. 106, pp. 252-257., 1984.

[10] Metzger, D. E., and Shepard, W. B., "Row Resolved Heat Transfer Variations in Pin Fin Arrays Including Effects of Non-Uniform Arrays and Flow Convergence," ASME Paper 86-GT-132., 1986.

[11] Chyu, M. K., "Heat Transfer and Pressure Drop for Short Pin-Fin Arrays with Pin-Endwall Fillet," *Journal of Heat Transfer*, vol. 112, pp. 926-932, 1990.

[12] Chyu, M. K., Hsing, Y. C., Shih, T.I.-P., and Natarajan, V.,"Heat Transfer Contributions of Pins and Endwall in Pin-Fin Arrays: Effects of Thermal Boundary Condition Modeling," Submitted in *ASME Turbo Expo '98*, Stockholm, June 205, 1998.

[13] Simoneau, R.J., and VanFossen, G. J.,"Effect of Location in an Array on Heat Transfer to a Short Cylinder in Crossflow," *ASME Journal of Heat Tranfer*, vol. 106, pp. 42-28, 1984.

[14] Al Dabagh, A. M., and Andrews, G. E.,"Pin-Fin Heat Transfer: Contribution of the Wall and the Pin to the Overall Heat Transfer," ASME Paper No.92-GT-242, 1992.

[15] Goldstein, R. J. and Jabbari, M. Y. and Chen, S.B.,"Convective Mass Transfer and Pressure Loss Characteristics of Staggered Short Pin Fin Arrays," International Journal of Heat and Mass Transfer,vol. 37, pp.149-160, 1994.

[16] Sparrow, E. M., Ramsey, J. M., and Altemani, C. A. C.,"Experiments on In-Line Pin Fin Arrays and Performance Comparisons with Staggered Arrays," *Journal*

of Heat Transfer, vol. 102, pp. 44-50, 1980.

[17] Kays, W. M., and Crawford, M. E., *Convective Heat and Mass Transfer*, McGraw-Hill, Inc., New York. 1993.

[18] Sparrow, E. M., Ramsey, J. M.,"Heat Transfer and Pressure Drop for a Staggered Wall-Attached Array of Cylinders with Tip Clearance," *International Journal of Heat and Mass Transfer*, vol. 21, pp. 1369-1377, 1978.

[19] Incropera, F. P., De Witt, D. P., *Introduction to Heat Transfer* Second Edition, John Wiley and Sons Inc., New York, 1990.

[20] Peng, Y.,"Heat Transfer and Frictional Loss Characteristics of Pin Fin Cooling Configuration," ASME Paper No.83-GT-123, 1983.

[21] Brigham, B. A., and VanFossen, G. J.,"Length to Diameter Ratio and Row Number Effects in Short Pin Fin Heat Transfer," *Journal of Heat Transfer*, vol. 106, pp. 241-245., 1984.

[22] Kline, S. J., and Mcklintock, F. A.,"Describing Uncertainties in Single Sample Experiments," *Mechanical Engineering*, vol. 75, Jan 1953.

APPENDIX A

NOMENCLATURE

A_{pin} pin fin cross sectional area, m^2

A_{plate} surface area of each copper plate, m^2

$A_{effective}$ exposed surface area of each copper plate, m^2

f friction factor

h average heat transfer coefficient, W/m^2

D_h hydraulic diameter

I current supplied to the heater, A

k_{air} thermal conductivity of air, W/(m.K)

k_{foam} thermal conductivity of foam, W/(m.K)

L length of the test section, m

$\bar{m}$ mass flow rate of air, kg/s

Nu overall average Nusselt number

Pr Prandtl number

Q rate of heat transfer by convection, W

Q_{loss} extraneous heat loss, W

Re_{Dh} Reynolds number

T_b bulk mean temperature, K

T_w average wall temperature, K

TP thermal performance ratio

V voltage across the heaters, V

Y expansion coefficient

Greek symbols

ρ density of air, kg/m^2

μ dynamic viscosity of air, $kg/(m.s)$

APPENDIX B

RAW DATA

The following is the raw data for case B for H/D=2.0, S_L/D=2.0 and S_T/D=2.0

H [in]	*1.0*	D_h	0.0457	k_{air}	0.0263
A_{cross}	0.0058	C_p	1007	k_{foam}	0.0350
A_{heated}	0.0523	m	1.85E-05	R	287
$d_{orifice}$	*1.50* in =0.0381 m				
d_{pipe}	*2.43* in =0.0617 m				
h	0.617				

Configs.	Case B		ST/D	2
	D [in]	0.5	SL/D	2
	H/D	2	# of Pins	76
	Aeff	0.0426	Aeff /Ah	0.8158
Re_{Dh}	26786	19573	12939	6675
TP	0.97	1.00	1.07	1.31
Nu_1/Nu_o	3.44	3.51	3.72	4.38
Nu_2/Nu_o	3.42	3.50	3.71	4.28
Nu_a/Nu_o	3.42	3.50	3.71	4.32
Nu_1	222	178	137	94
Nu_2	221	178	136	92
Nu_a	222	178	137	93
f	1.96	2.06	2.25	2.29
f/f_o	80	79	77	65
Nu_1^*/Nu_o	4.21	4.30	4.56	5.37
Nu_2^*/Nu_o	4.19	4.29	4.55	5.25
Nu_a^*/Nu_o	4.20	4.29	4.55	5.29
Nu_1^*	273	218	168	115
Nu_2^*	271	218	167	113
Nu_a^*	272	218	167	114
h_1	128	102	79	54
h_2	127	102	79	53
h_{ave}	127	102	79	53
Nu_o	65	51	37	21
f_o	0.02	0.03	0.03	0.04
q_{conv}	128.51	99.86	76.34	47.16
q_{loss}	0.96	0.94	0.94	0.87
T_{in}	23.20	23.00	23.05	23.35
$T_{m,\,1}$	23.54	23.36	23.47	23.85

$T_{m,\,2}$	24.22	24.08	24.30	24.85
$T_{w,\,1}$	42.76	42.01	42.05	40.51
$T_{w,\,2}$	43.54	42.77	42.91	41.90
V_{in}	9.31	6.80	4.50	2.32
m_{dot}	0.06	0.05	0.03	0.02
C	0.61	0.61	0.62	0.62
Y	0.99	0.99	1.00	1.00
p_o [Pa]	99972	100569	100972	101216
Dp_o [Pa]	2997	1567	671	174
Dp [Pa]	547	308	147	40
$\|p_o\|$ [in]	5.40	3.00	1.38	0.40
Dp_o [in]	12.05	6.30	2.70	0.70
Dp [in]	2.20	1.24	0.59	0.16
V	47.60	42.00	36.80	29.11
I	2.72	2.40	2.10	1.65
$T_{in,\,1}$	23.40	22.90	23.00	23.50
$T_{in,\,2}$	23.00	23.10	23.10	23.20
T_1	42.65	41.89	41.96	40.45
T_2	42.81	42.05	42.10	40.57
T_3	42.82	42.06	42.10	40.57
T_4	42.70	41.92	41.97	40.44
T_5	42.81	42.03	42.04	40.47
T_6	42.49	41.72	41.76	40.21
T_7	43.10	42.26	42.25	40.63
T_8	42.70	41.98	42.03	40.50
T_9	43.11	42.39	42.45	40.94
T_{10}	42.58	41.86	41.91	40.39
T_{11}	42.61	41.91	41.96	40.45
T_{12}	43.51	42.75	42.92	41.95
T_{13}	43.45	42.63	42.76	41.73
T_{14}	44.00	43.21	43.33	42.32
T_{15}	43.70	42.89	43.02	41.99
T_{16}	43.55	42.73	42.82	41.79
T_{17}	43.34	42.52	42.63	41.59
T_{18}	43.26	42.43	42.54	41.49
T_{19}	43.84	43.09	43.21	42.20
T_{20}	43.60	42.88	43.04	42.05
T_{21}	43.36	42.63	42.78	41.76
T_{22}	43.37	42.73	42.94	42.02

APPENDIX C

UNCERTAINTY ANALYSIS

The uncertainty analysis is based on a confidence level of 95% and are based on Kline Mcklintock method [18]. The uncertainty values of the Nusselt number. A sample uncertainty is shown below.

The uncertainty for mass flow rate $\dot{m}$ was calculated as follows

$$\dot{m} = \frac{\pi}{4} {d_0}^2 CY \left[\frac{p_0 \Delta p_0}{RT_0(1-\eta^4)} \right]^{1/2} \tag{C.1}$$

where d_o, C, Y, and η may be considered to be constants

and hence

$$\frac{U_{\dot{m}}}{\dot{m}} = \left[\left(\frac{1}{2} \frac{U_{p_o}}{p_o} \right)^2 + \left(\frac{1}{2} \frac{U_{\Delta p_o}}{\Delta p_o} \right)^2 + \left(\frac{-1}{2} \frac{U_{T_o}}{T_o} \right)^2 \right]^{1/2} \tag{C.2}$$

The uncertainties of the Reynolds number and the Nusselt number are estimated at $\pm 5.39\%$ and $\pm 3.45\%$ respectively

VITA

Vamsee Satish Achanta was born in Kakinada, India on July 28, 1980. He received his Bachelor of Technology degree in Mechanical Engineering from Indian Institute of Technology, Madras, India in May 2001. The author may be contacted at 70-2-115, Near Nookalamma Temple, Ramanayya Peta, Kakinada, Andhra Pradesh, India, 533003 or by email at satish_va@yahoo.com and achanta@neo.tamu.edu.

The typist for this thesis was Vamsee Satish Achanta.